PERGAMON

International Journal of Heat and Mass Transfer 43 (2000) 1573–1589

International Journal of HEAT and MASS TRANSFER

www.elsevier.com/locate/ijhmt

Entrainment and desposition rates of droplets in annular two-phase flow

I. Kataoka[a], M. Ishii[b,*], A. Nakayama[c]

[a]*Department of Mechanophysics Engineering, Osaka University, Suita, Osaka 565-0871, Japan*
[b]*Department of Nuclear Engineering, Purdue Univeristy, West Lafeyette, IN 47907-1290, USA*
[c]*Department of Mechanical Engineering, Kyushu Sangyo University, Fukuoka 813-8503, Japan*

Received 28 May 1998; received in revised form 14 July 1999

Abstract

The droplet entrainment from a liquid film is important to the mass, momentum, and energy transfer process in annular two-phase flow. For example, the amount of entrainment as well as the rate of entrainment significantly affect the occurrences of the dryout, whereas the post CHF heat transfer depends strongly on the entrainment and droplet sizes. Despite the importance of the entrainment rate, there have been no satisfactory correlations available in the literature. In view of these, correlations for entrainment rate covering both entrance region and equilibrium region have been developed from a simple model in collaboration with data. Results show that the entrainment rate varies considerably in the entrainment development region. However, at a certain distance from an inlet it attains an equilibrium value. A simple approximate correlation has been obtained for the equilibrium state where entrainment rate and deposition rate become equal. The result indicates that the equilibrium entrainment rate is proportional to Weber number based on the hydraulic diameter of a tube.

1. Introduction

The droplet entrainment rate from a liquid film is important in analyzing heat and mass transfer processes in annular two-phase flow. Mass, momentum and energy transfer processes are strongly affected by the amount of droplets in the streaming gas [1,2]. The amount of droplet entrainment is determined by the integral balance between the droplet entrainment rate and the droplet deposition rate. In particular, the accurate knowledge of entrainment is indispensable for the prediction of the dryout and post dryout heat transfer [3–8] and the effectiveness of the emergency core cooling in light water reactors [9–12].

Based on the mechanistic model of shearing off of roll-waves by the streaming gas, correlations for the inception of droplet entrainment [13], amount of entrained droplets for a steady state flow [2], and droplet size and its distributions [14] have been developed recently. As for a deposition rate of droplets in a streaming gas, there have been many experimental and theoretical works and satisfactory correlations have been developed [1,15–28]. However, the process of the entrainment seems more complicated and thus the efforts to develop a reliable entrainment rate correlation have not been very successful. The lack of such a correlation has been the main difficulty of a detailed analysis of various phenomena in transient annular two-phase flow or in a post dryout regime. The main objective of this paper is to develop a reliable correlation for entrainment rate from the liquid film. In the case of LWR transients and accidents, annular flow or

* Corresponding author. Tel.: +1-765-494-4587; fax: +1-765-494-9570.

0017-9310/00/$ - see front matter
PII: S0017-9310(99)00236-7

Nomenclature

C	Droplet concentration in gas core
C_∞	Equilibrium droplet concentration in gas core
$\dot{d}$	Droplet deposition rate
D	Hydraulic diameter
E	Fraction of liquid flux flowing as droplet ($= j_{fe}/j_f$)
E_∞	Equilibrium value of fraction entrained, E
g	Acceleration due to gravity
j_f	Volumetric flux of total liquid (superficial velocity)
j_{fe}	Volumetric flux of droplets
j_g	Volumetric flux of gas (superficial velocity)
k	Mass transfer coefficient
Re_f	Total liquid Reynolds number
Re_{ff}	Liquid film Reynolds number
$Re_{ff\infty}$	Equilibrium film Reynolds number
Re_g	Gas Reynolds number
v_{ff}	Liquid film velocity
$v_{ff\infty}$	Equilibrium liquid film velocity
v_{fe}	Velocity of droplets
v_g	Gas velocity
We	Entrainment Weber number defined by Eq. (19)
W_f	Total liquid mass flow rate
W_{fe}	Droplet mass flow rate
z	Axial distance from inlet

Greek symbols

α	Void fraction
α_{core}	Fraction of gas core
α_d	Droplet fraction in the gas core
δ	Film thickness
$\dot{\varepsilon}$	Entrainment rate
$\dot{\varepsilon}_\infty$	Equilibrium entrainment rate
ζ	Dimensionless distance given by Eq. (24)
μ_f	Viscosity of liquid
μ_g	Viscosity of gas
ρ_f	Liquid density
ρ_g	Gas density
$\Delta\rho$	Density difference between liquid and gas
σ	Surface tension
τ_i	Interfacial shear force

Subscripts

f	Liquid phase
fe	Liquid entrainment
ff	Liquid film
g	Gas phase
i	Interface
∞	Equilibrium

droplet flow may be encountered under various conditions. Therefore, a general correlation covering a wide range of flow conditions including entrance effects is highly desirable. As a first step, an entrainment rate correlation has been developed for relatively low viscous fluid such as water where the entrainment of droplets is generated mainly by the shearing-off of roll wave crests.

2. Previous works

In annular two-phase flow for low viscous fluid and for relatively high film Reynolds number ($Re_f \geq 160$), the mechanism of entrainment is basically the shearing-off of roll wave crests by a highly turbulent gas flow [13,19].

Based on the modeling of this mechanism, an onset of entrainment criterion [13] and a correlation for the amount of entrained droplet [2] have been developed. After establishing the basic parameters governing the entrainment process, the correlation has been obtained in collaboration with a large number of data. In addition to being accurate under steady state conditions, this correlation also indicated basic mechanisms of entrainment processes and parametric dependencies. A correlation for entrainment in the entrance region and for the necessary distance for the development of entrainment have been obtained [2]. These supply valuable information on the process of entrainment. Detailed reviews of the other correlations for the amount of droplet entrainment have been given by Hewitt and Hall-Taylor [1] and Ishii and Mishima [2].

The amount of entrained droplets represents the integral effects of the rate processes of entrainment and deposition. Therefore, it is considered that the amount of entrainment is a more stable parameter to measure and correlate than the entrainment rate. However, the above discussed correlation is suitable to quasi steady state conditions and under certain transient conditions its application can lead to considerable errors. From this point of view, Hutchinson and Whalley [31] and Whalley et al. [32] developed the entrainment rate correlation. The deposition rate d can be linearly related to the droplet concentration in the gas core by

$$\dot{d} = kC \tag{1}$$

where k is the mass transfer coefficient and C is the droplet mass concentration in the gas core. Therefore, the entrainment rate has been related to the equilibrium concentration C_∞ by

$$\dot{\varepsilon} = kC_\infty \tag{2}$$

Then the equilibrium concentration has been correlated by

$$C_\infty = C_\infty\left(\frac{\tau_i\delta}{\sigma}\right) \tag{3}$$

where τ_i, δ and σ are the interfacial shear, film thickness, and surface tension, respectively.

Although this correlation method is conceptually right and is more mechanistic than the correlation for the amount of entrainment, there are some difficulties associated with it. The first one is related to the development of the correlation for the equilibrium concentration C_∞. The data showed considerable scattering which can be up to more than one order of magnitude, particularly at small values of $\tau_i\delta/\sigma$. This suggests that a single dimensionless group used to correlate C_∞ is not sufficient. Furthermore, in many entrainment experiments such parameters as C_∞ and δ are not measured directly, thus some modeling to deduce data to useful forms has been necessary.

Ueda [33] presented the entrainment rate correlation in a similar manner as the above mentioned correlation. His correlation is dimensional and given by

$$\dot{\varepsilon} = 3.54\times10^{-3}\left\{\frac{\tau_i}{\sigma}\left(\frac{j_f}{\sigma}\right)^{0.60}\right\}^{0.57} \tag{4}$$

for

$$\frac{\tau_i}{\sigma}\left(\frac{j_f}{\sigma}\right)^{0.60} \geq 120 \tag{5}$$

where $\dot{\varepsilon}$ is in kg/m^{2}s, τ_i in N/m^2. σ in N/m and j_f in m/s. Although Eq. (4) correlates his experimental data, it is dimensional and parameter (j_f/σ) is not based on physical mechanisms of entrainment. Therefore, it is expected that the correlation may not apply to general cases.

It can be said that existing correlations for entrainment rate are not satisfactory. However, the entrainment and deposition rates are more mechanistic parameters representing the true transfer of mass at the wavy interfaces than the entrainment fraction. Particularly for analyzing the entrance and developing flow regions or transient flow, an accurate entrainment rate correlation is indispensable. In view of the highly reliable correlation for the amount of entrainment [2] which has been developed previously from a simple modeling, it has been thought that a sufficient understanding of the entrainment mechanism exists to extend the model to the rate processes of entrainment. Thus, an attempt has been made to develop an entrainment rate correlation based on physical modeling in this study.

3. Basic equation for entrainment rate

For annular dispersed two-phase flow one may write the following mass balance equation at the interface under steady state and without phase change conditions.

$$\dot{\varepsilon} = \frac{D\rho_f j_f}{4}\left(\frac{\partial E}{\partial z}\right) + \dot{d} \tag{6}$$

where $\dot{\varepsilon}$ and $\dot{d}$ are entrainment rate and deposition rate per unit interfacial area (in kg/m^2 s), respectively, and z is a distance from inlet. E is the entrainment fraction defined as

$$E = \frac{W_{fe}}{W_f} = \frac{j_{fe}}{j_f} \tag{7}$$

where W_{fe}, W_f, j_{fe} and j_f are droplet mass flow rate, total liquid mass flow rate, droplet volumetric flux, and total liquid volumetric flux, respectively.

Deposition rate for the diffusion controlled deposition process may be given approximately by

$$\dot{d} \cong kC \tag{8}$$

where C is the droplet concentration in the core and k is the mass transfer coefficient. There have been many theoretical and experimental works on the mass transfer coefficient k and several reliable correlations have been developed [15–28].

Among these correlations the correlation of Namie and Uneda [25,26] is the most general one when droplets have no large initial velocity and are controlled by turbulent diffusion. Their correlation is based on detailed physical analysis of flow structure, turbulent diffusivity of gas and droplets, and effect of droplet diameter. However, it is too complicated to apply to the present analysis. The correlation of Paleev and Filippovich [19] has similar functional form and agrees well with the correlation of Namie and Ueda [25,26] in average over droplet diameter. The former can be regarded as the simplified correlation of the latter. Therefore, in the present analysis, Paleev and Filipovich's correlation [19] is used. Their correlation is given by

$$\frac{k}{j_g} - 0.022 Re_g^{-0.25} \left(\frac{C}{\rho_f}\right)^{-0.26} \left(\frac{\rho_g}{\rho_f}\right)^{0.26} \tag{9}$$

where $Re_g \equiv \rho_g j_g D/\mu_g$. On the other hand, the droplet mass concentration C, which is the droplet mass per unit mixture volume, is defined by the following expression.

$$C = \rho_f \frac{j_{fe} v_g}{j_g v_{fe} + j_{fe} v_g} \tag{10}$$

or by introducing the entrainment fraction $E = j_{fe}/j_f$,

$$C = \frac{\rho_f E j_f v_g / (j_g v_{fe})}{1 + E j_f v_g / (j_g v_{fe})} \tag{11}$$

Assuming that the droplet velocity in the gas core is approximately equal to the gas velocity, Eq. (11) can be simplified to

$$C \cong \rho_f \frac{E\frac{j_f}{j_g}}{1 + E\frac{j_f}{j_g}} \tag{12}$$

In annular two-phase flow, the liquid volumetric flux is much less than the gas volumetri flux, that is

$$\frac{j_f}{j_g} \ll 1 \tag{13}$$

Furthermore, since E is between 0 and 1,

$$E\frac{j_f}{j_g} \ll 1 \tag{14}$$

Then Eq. (12) is approximated by

$$C \cong \rho_f E \frac{j_f}{j_g} \tag{15}$$

From Eqs. (8), (9) and (15), the deposition rate correlation can be simplified to

$$\frac{\dot{d}}{\rho_f j_f} = 0.022 Re_g^{-0.25} \left(E\frac{j_f}{j_g}\right)^{0.74} \left(\frac{j_g}{j_f}\right) \left(\frac{\rho_g}{\rho_f}\right)^{0.26}$$

$$\cong 0.022 Re_f^{-0.26} \left(\frac{\mu_g}{\mu_f}\right)^{0.26} E^{0.74} \tag{17}$$

By substituting Eq. (17) into Eq. (6), the entrainment rate becomes

$$\dot{\varepsilon} = \frac{D\rho_f j_f}{4} \left(\frac{\partial E}{\partial z}\right) + 0.022 \rho_f j_f Re_f^{-0.26} \left(\frac{\mu_g}{\mu_f}\right)^{0.26} E^{0.74} \tag{18}$$

Eq. (18) indicates that knowing the entrainment fraction distribution along the flow direction, one can calculate the entrainment rate. In the following sections, entrainment rate is calculated from the existing entrainment fraction correlation in collaboration with experimental data.

4. Entrainment rate correlation

Ishii and Mishima [2] developed a correlation for entrainment fraction based on the mechanistic model of shearing-off of roll wave crest by a streaming gas. The fraction of liquid flux flowing as droplets, E, is correlated in terms of two dimensionless groups given by:

Weber number for entrainment

$$We = \frac{\rho_g j_g^2 D}{\sigma} \left(\frac{\Delta\rho}{\rho_g}\right)^{1/3} \tag{19}$$

Total liquid Reynolds number

$$Re_f = \frac{\rho_f j_f D}{\mu_f} \tag{20}$$

The entrained fraction reaches a quasi-equilibrium value E_∞, at points far removed from the tube entrance where the entrainment and deposition processes attain an equilibrium condition. The distance necessary to reach this condition is given approximately by

$$z = \frac{440 D We^{0.25}}{Re_f^{0.5}} \tag{21}$$

for cases with smooth liquid injection. At this entrance length the entrainment has reached within about 2% of its ultimate value. Then for the region $z \geq 440 D We^{0.25}/Re_f^{0.5}$ the correlation becomes

$$E \cong E_\infty = \tanh\left(7.25 \times 10^{-7} We^{1.25} Re_f^{0.25}\right) \tag{22}$$

This correlation has been compared to many experimental data for air–water systems in the ranges of $1 < p < 4$ atm, $0.95 < D < 3.2$ cm, $370 < Re_f < 64000$, and $j_g < 100$ m/s, and the result has shown to be satisfactory. The various parametric dependencies have been explained in terms of physical mechanisms.

Some experimental data indicated the strong entrance effect as well as the gas expansion effect due to the axial pressure drop in a low pressure system. For the correlation development it was essential to use a local gas velocity or volumetric flux based on a local pressure in evaluating data. By separating these two effects, an additional correlation for the entrance effect on entrainment have been developed. As mentioned

above, the entrance region is given by $0 < z < 440DWe^{0.25}/Re_f^{0.5}$. The correlation takes a typical form of an exponential relaxation, and it essentially reaches the quasi-equilibrium value given by E_∞ for large values of z. Thus, for the case of liquid being injected smoothly as a film at inlet, the entrainment develops according to

$$E = \left(1 - \exp\left(-1.87 \quad \times 10^{-5}\zeta^2\right)\right)E_\infty \tag{23}$$

Here ζ is the dimensionless distance given by

$$\zeta = \frac{(z/D)Re_f^{0.5}}{We^{0.25}} \tag{24}$$

Because of the nature of the above equation this correlation is not limited to the entrance region, but it can be used as a general correlation everywhere. A number of data from the entrance region have been successfully correlated by this expression.

The above entrainment fraction correlation can be used to evaluate the value of E as well as the dependency of E on z in Eq. (18). Thus by substituting Eq. (23) into Eq. (18), one obtains

$$\begin{aligned}\dot{\varepsilon} = {} & 0.935 \times 10^{-5}\zeta \exp\left(-1.87\right. \\ & \left.\times 10^{-5}\zeta^2\right)\rho_f j_f Re_f^{0.5} We^{-0.25} E_\infty \\ & + 0.022\rho_f j_f Re_f^{-0.26}\left(\frac{\mu_g}{\mu_f}\right)^{0.26} E_\infty^{0.74} \\ & \times \left(1 - \exp\left(-1.87 \times 10^{-5}\zeta^2\right)\right)^{0.74}\end{aligned} \tag{25}$$

Fig. 1 shows entrainment rate calculated by Eq. (25) for air–water systems and $We = 2000$ and $Re_f = 100$–10,000. In the above correlation, the entrainment rate is expressed in terms of the operational conditions and the distance from the entrance. However, for a truly universal entrainment rate correlation, it is desirable that the $\dot{\varepsilon}$ is expressed by local flow conditions alone rather than by a combination of the operational conditions and the axial location. For this purpose several modifications are made on the above equation by taking account of some important limiting conditions.

By considering a quasi-equilibrium region where $\zeta < 1$, the above equation can be reduced to the expression for equilibrium entrainment rate $\dot{\varepsilon}_\infty$ as

$$\dot{\varepsilon}_\infty = 0.022\rho_f j_f Re_f^{-0.26}\left(\frac{\mu_g}{\mu_f}\right)^{0.26} E_\infty^{0.74} \tag{26}$$

By rearranging the above equation, one can obtain

$$\frac{\dot{\varepsilon}_\infty D}{\mu_f} = 0.022 Re_f^{0.74}\left(\frac{\mu_g}{\mu_f}\right)^{0.26} E_\infty^{0.74} \tag{27}$$

Since $\dot{\varepsilon}_\infty$ is the mass flux normal to an interface due to entrainment, $\dot{\varepsilon}_\infty D/\mu_f$ can be considered as the entrainment Reynolds number.

The above equation shows that the rate of entrainment depends on the total liquid Reynolds number, viscosity ratio, and entrainment fraction E_∞. The fraction of entrainment under a quasi-equilibrium condition is given by Eq. (22) which shows the dependence of E_∞ on We and total liquid Reynolds number Re_f. However, it is also possible to interpret the existence of E_∞ in Eq. (27) as representing the local dynamical condition at the interface. In that case, it is more meaningful to rewrite the expression for E_∞, Eq. (22), in terms of the local film Reynolds number defined by

$$Re_{ff} \equiv \frac{\rho_f j_{ff} D}{\mu_f} \tag{28}$$

where j_{ff} is the film liquid volumetric flux. Since by definition $j_f = j_{fe} + j_{ff}$ and $j_{ff} = j_f(1 - E)$, one obtains

$$Re_{ff\infty} = Re_f(1 - E_\infty) \tag{29}$$

and

$$Re_{ff} = Re_f(1 - E) \tag{30}$$

where ∞ denotes the equilibrium condition.

By substituting Eq. (29) into Eq. (22),one gets

$$E_\infty = \tanh\left(7.25 \times 10^{-7} We^{1.25} Re_{ff\infty}^{0.25}/(1 - E_\infty)^{0.25}\right) \tag{31}$$

Thus

$$7.25 \times 10^{-7} We^{1.25} Re_{ff\infty}^{0.25} = \frac{1}{2}(1 - E_\infty)^{0.25}\ln\left(\frac{1 + E_\infty}{1 - E_\infty}\right) \tag{32}$$

However, it is easy to show that the right-hand side of Eq. (32) can be approximated as

$$\frac{1}{2}(1 - E_\infty)^{0.25}\ln\left(\frac{1 + E_\infty}{1 - E_\infty}\right) = 0.9355E_\infty \tag{33}$$

for a wide range of E_∞ from 0 up to 0.97. Then, from Eqs. (32) and (33) one obtains

$$E_\infty = 7.75 \times 10^{-7} We^{1.25} Re_{ff\infty}^{0.25} \tag{34}$$

By eliminating E_∞ between Eqs. (27) and (34), the rate of entrainment becomes

$$\frac{\dot{\varepsilon}_\infty D}{\mu_f} = 6.6 \times 10^{-7} Re_f^{0.74} Re_{ff\infty}^{0.185} We^{0.925}\left(\frac{\mu_g}{\mu_f}\right)^{0.26} \tag{35}$$

The above correlation shows that the entrainment rate

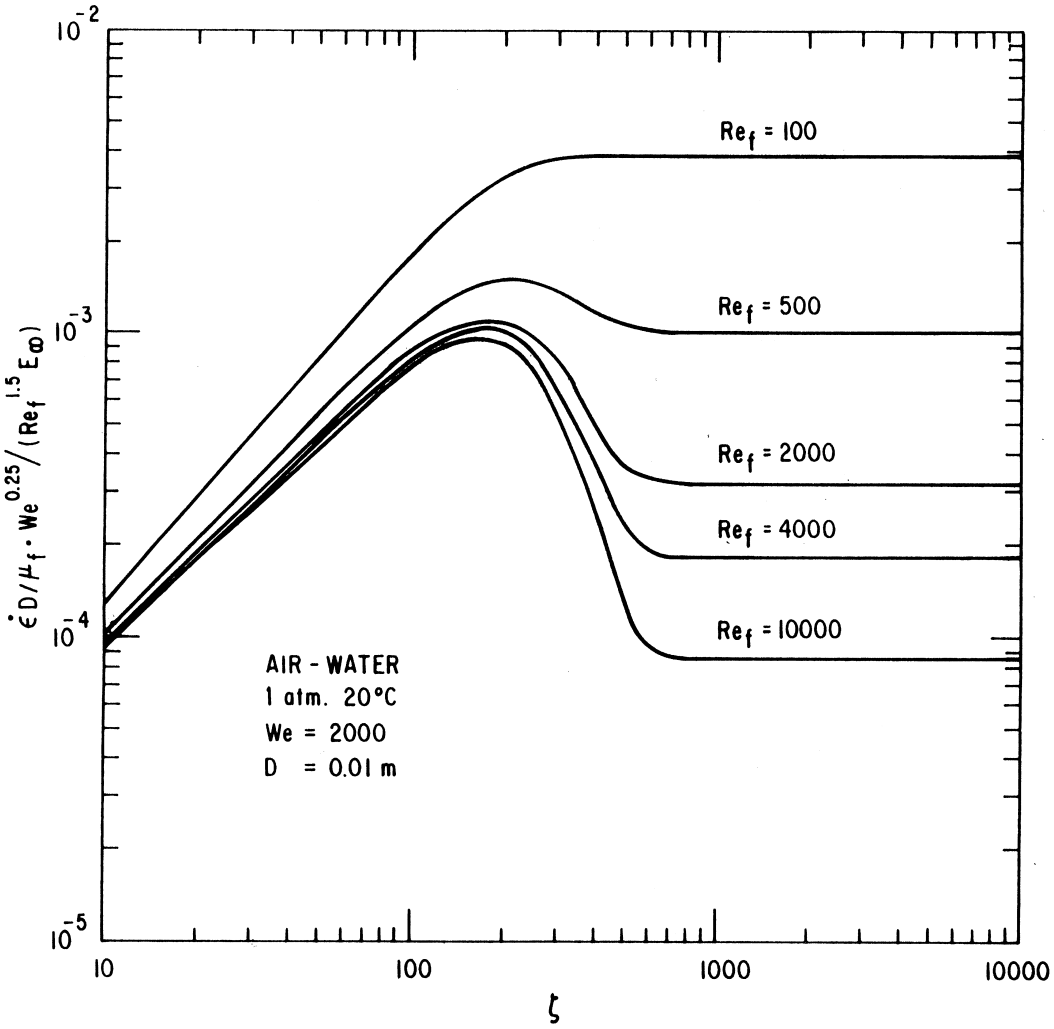

Fig. 1. Entertainment rate calculated by Eq. (25) for $We = 2000$, $Re_f = 100$–10,000, and $D = 0.01$ m in air–water system at 20°C, 1 atm.

depends on the total liquid Reynolds number, local film Reynolds number, local Weber number based on the hydraulic diameter, and the viscosity ratio. This correlation has been developed from the equilibrium entrainment fraction and deposition rate correlations. Although these correlations are based on steady state data, several observations can be made. Except at the entrance region, the entrainment and deposition processes may be considered as local phenomena which can be determined by the local parameters. Hence, if the rate correlations are expressed in terms of local parameters such as the local film Reynolds number and droplet mass concentration, it is expected that these correlations may be extended to nonequilibrium or unsteady conditions.

Based on this hypothesis which is commonly accepted except in very rapid transient situations, the equilibrium entrainment rate correlation is extended to more general case except at the entrance region. Thus, replacing $\dot{\varepsilon}_\infty$ by $\dot{\varepsilon}$ in Eq. (35), the general entrainment rate correlation is given by

$$\frac{\dot{\varepsilon} D}{\mu_f} = 6.6 \times 10^{-7} Re_f^{0.74} Re_{ff}^{0.185} We^{0.925} \left(\frac{\mu_g}{\mu_f}\right)^{0.26} \tag{36}$$

for regions away from the entrance, i.e., $z > 440 D We^{0.25}/Re_f^{0.5}$.

The above correlation indicates that the entrainment rate is roughly proportional to the effective Weber number based on the hydraulic diameter and to the liquid Reynolds number. These appear to correctly reflect the true physical mechanism of entrainment. The entrainment under consideration is caused by shearing-off of roll wave crests by gas core flow. There-

fore, it is expected that the entrainment rate is proportional to an interfacial drag force or to j_g^2. The drag force is also proportional to roughness of the interface or the wave amplitude which may be related to the liquid Reynolds numbers. The correlation given by Eq. (36) indicates that $\dot{\varepsilon} \sim Re_f^{0.925}$ when the entrainment fraction is small. However, as the entrainment increases the liquid film Reynolds number should decrease. The expected decrease in the entrainment rate as the film becomes thinner is reflected on the dependence of $\dot{\varepsilon}$ on Re_{ff}. At the limiting case of $Re_{ff} \to 0$, the correlation predicts the right limit of $\dot{\varepsilon} \to 0$.

Although, as a first approximation, Eq. (36) can also be used in the entrance region, a more careful study on the transient and memory effects are needed. From this point of view, the entrainment rate in the entrance region and the validity of this correlation in the entrance region are studied in the next section.

5. Entrainment rate in entrance region

5.1. General formulation of entrainment rate

The correlation for entrainment at the entrance section given by Eq. (25) is developed for the case of the smooth injection of liquid as a film. In this particular case, the amount of entrainment gradually increases from zero to the equilibrium value with the distance from the inlet. From this entrainment correlation the rate of entrainment can be obtained. Although this rate applies only to the case with excess liquid on the film, compared to the equilibrium condition, the generalization of the model can be possible and will be discussed later.

From Eq. (23) the nondimensional distance parameter ζ can be expressed in terms of E/E_∞ as

$$\varsigma = 231\sqrt{\ln\left(\frac{1}{1-E/E_\infty}\right)} \tag{37}$$

by eliminating ζ in Eq. (25) in view of Eq. (37), and using Eq. (34), one obtains

$$\begin{aligned}\frac{\dot{\varepsilon}D}{\mu_f} &= 1.67\times10^{-9} Re_f^{1.5} Re_{ff\infty}^{0.25} We \sqrt{\ln\frac{1}{(1-E/E_\infty)}} \\ &\times\left(1-\frac{E}{E_\infty}\right) + 6.6\times10^{-7} Re_f^{0.74} Re_{ff\infty}^{0.185} \\ &\times We^{0.925}\left(\frac{\mu_g}{\mu_f}\right)^{0.26}\left(\frac{E}{E_\infty}\right)^{0.74}\end{aligned} \tag{38}$$

As shown in Fig. 1, because of the existence of the first term on the right-hand side, Eq. (38) gives much higher values of the entrainment rate than Eq. (36) for large Re_f and We in the entrance region where $E/E_\infty < 1$. This figure is the contribution of the first term of the right-hand side of Eq. (38). It is attributed to excess kinetic energy of the film over the equilibrium state discussed later. The above rate correlation is a rather complicated function of E/E_∞, therefore, some modifications are made to obtain a simplified correlation in the entrance region. By considering the entrainment rate in the entrance region, where $E/E_\infty < 1$, as a function of E/E_∞, one can assume the following functional form for the entrainment rate.

$$\frac{\dot{\varepsilon}D}{\mu_f} = f(E/E_\infty) + \left(\frac{\dot{\varepsilon}D}{\mu_f}\right)_\infty \tag{39}$$

where the equilibrium rate is given by Eq. (36).

Since $\dot{\varepsilon}$ approaches $\dot{\varepsilon}_\infty$ when $E/E_\infty \to 1$, $f(E/E_\infty)$ must approach zero as $E/E_\infty \le 1$. Furthermore, $f(E/E_\infty)$ is an additional term which should appear only for an entrance region where $E/E_\infty \le 1$. In other words, $f(E/E_\infty)$ should be zero when the entrainment exceeds that of the equilibrium value. Hence

$$\begin{cases} f(E/E_\infty) = 0 & \text{for } E/E_\infty > 1 \\ f(1) = 0 \end{cases} \tag{40}$$

The above two conditions can be explained in terms of the entrainment mechanisms as follows. When the liquid film flow is above the equilibrium value, i.e., $Re_{ff} > Re_{ff\infty}$, there is an extra entrainment force in addition to the equilibrium rate expressed by Eq. (36). The excess liquid flow in the film or $(Re_{ff} - Re_{ff\infty})$ acts as a driving force to promote the entrainment.

The exact form of the function $f(E/E_\infty)$ based on the entrainment correlation of Ishii and Mishima [2] is derived from Eqs. (23), (24) and (34) and is given by

$$\begin{aligned} f(E/E_\infty) &= 1.67\times10^{-9} Re_f^{1.5} Re_{ff\infty}^{0.25} \\ &\times We\sqrt{\ln\frac{1}{(1-E/E_\infty)}}\left(1-\frac{E}{E_\infty}\right)\end{aligned} \tag{41}$$

Several observations can be made with respect to Eq. (41). The function $f(E/E_\infty)$ is zero at $E = 0$ and E_∞ has a maximum at $E/E_\infty = 0.4$. Thus

$$\max(f) = 0.718\times10^{-9} Re_f^{1.5} Re_{ff\infty}^{0.25} We \tag{42}$$

This occurs at $\zeta \cong 160$. It indicates that the extra entrainment force is very small for extremely low values of E. Some experimental data support the existence of this very small value of $f(E/E_\infty)$ at the vicinity of the inlet as shown in the following discussion of experimental data. This low level of entrainment at high

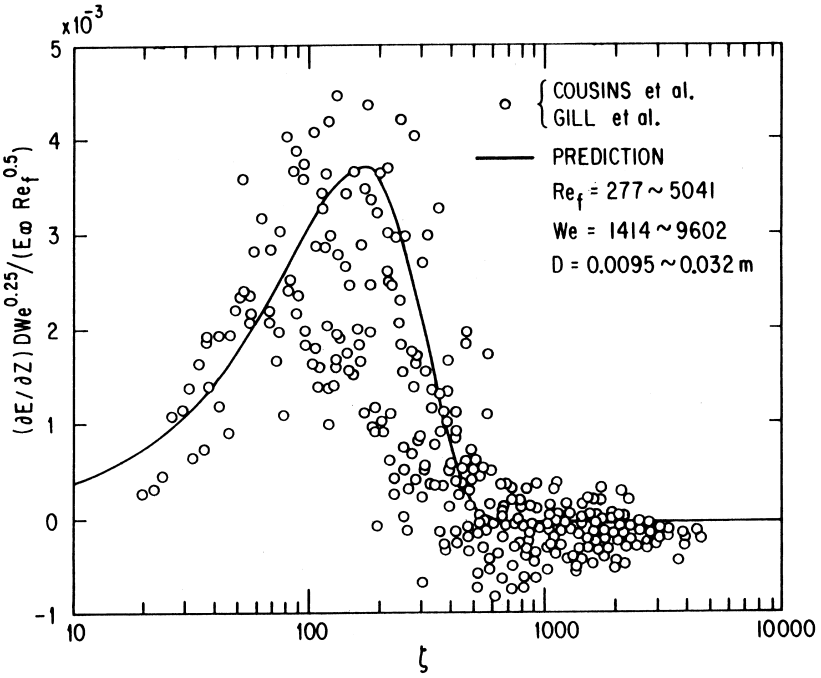

Fig. 2. $\frac{\partial E}{\partial z} DWe^{0.25}/E_\infty Re_f^{0.5}$ vs. ζ for the data of Cousin et al. [18] and Gill et al. [17].

liquid film flow at the entrance may be attributed to the finite distance needed for the development of interfacial waves and entrainment. However, because of this, the entrainment mechanism in this region is strongly dependent on the geometry of the inlet itself.

In view of the above, the vicinity of the inlet is neglected in the following simple model development. It is assumed that the function $f(E/E_\infty)$ takes the maximum value at $E/E_\infty \to 1$ and the function is approximated by the following form.

$$f(E/E_\infty) = \begin{cases} 0.718 \times 10^{-9} Re_f^{1.5} Re_{ff\infty}^{0.25} We \left(1 - \dfrac{E}{E_\infty}\right)^2 & \text{for } E/E_\infty \le 1 \\ 0 & \text{for } E/E_\infty \le 1 \end{cases} \quad (43)$$

This form indicates that the driving force for this extra entrainment is $(1 - E/E_\infty)^2$. Thus the value of $f(E/E_\infty)$ is higher for a larger deviation of E from the equilibrium value E_∞.

Substituting Eqs. (36) and (43) into Eq. (39), and using the relation $Re_{ff} = Re_f(1 - E)$, one finally obtains the entrainment rate correlation for $E/E_\infty \le 1$ given by

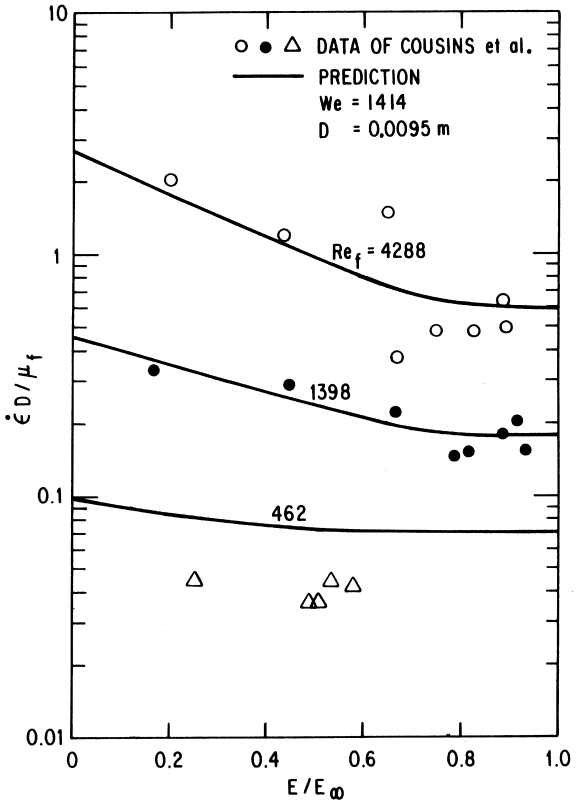

Fig. 3. Entertrainment rate for the data of Cousion et al. [18] at $We = 1414$ and $Re_f = 462$–4288.

$$\frac{\dot{\varepsilon}D}{\mu_f} = 0.72 \times 10^{-9} Re_f^{1.75} We(1-E_\infty)^{0.25} \times \left(1-\frac{E}{E_\infty}\right)^2 + 6.6 \times 10^{-7}(Re_f We)^{0.925} \times \left(\frac{\mu_g}{\mu_f}\right)^{0.26}(1-E)^{0.185} \quad (44)$$

and for $E/E_\infty > 1$ by

$$\frac{\dot{\varepsilon}D}{\mu_f} = 6.6 \times 10^{-7}(Re_f We)^{0.925}\left(\frac{\mu_g}{\mu_f}\right)^{0.26}(1-E)^{0.185} \quad (45)$$

where E_∞ is given by Eq. (31)

However, from Eqs. (29), (30) and (31), it can be shown that

$$\left(1-\frac{E}{E_\infty}\right) = \frac{Re_{ff} - Re_{f\infty}}{7.75 \times 10^{-7} We^{1.25} Re_{ff\infty}^{0.25} Re_f} \quad (46)$$

where Re_{ff} and $Re_{ff\infty}$ are the local film Reynolds number and the equilibrium film Reynolds number, respectively. Hence by substituting Eq. (46) into Eq. (44) the entrainment rate correlations can be expressed in terms of the liquid film Reynolds numbers as follows. For $Re_{ff} \geq Re_{ff\infty}$

$$\frac{\dot{\varepsilon}D}{\mu_f} = 1.2 \times 10^3 Re_f^{-0.5} Re_{ff\infty}^{-0.25} We^{-1.5}(Re_{ff} - Re_{ff\infty})^2 + 6.6 \times 10^{-7} Re_f^{0.74} Re_{ff}^{0.185} We^{0.925}\left(\frac{\mu_g}{\mu_f}\right)^{0.26} \quad (47)$$

And for $Re_{ff} < Re_{ff\infty}$

$$\frac{\dot{\varepsilon}D}{\mu_f} = 6.6 \times 10^{-7} Re_f^{0.74} Re_{ff}^{0.185} We^{0.925}\left(\frac{\mu_g}{\mu_f}\right)^{0.26} \quad (48)$$

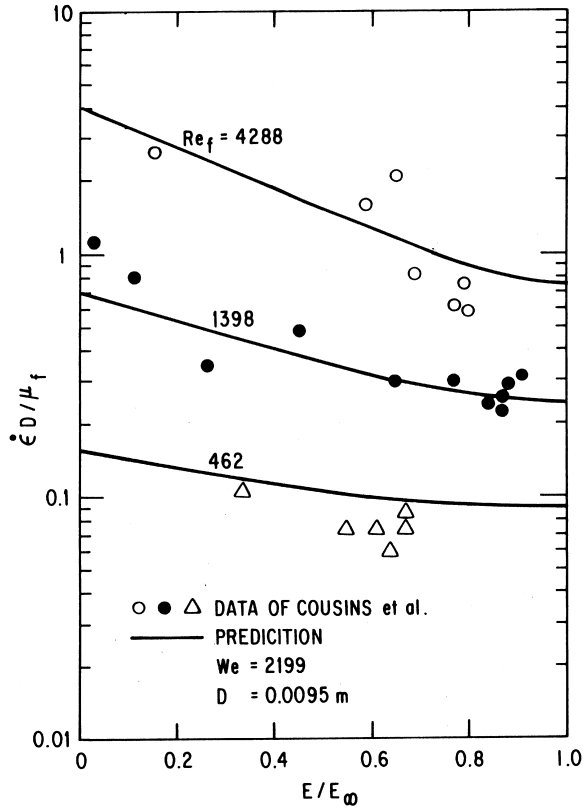

Fig. 4. Entertrainment rate for the data Cousins et al. [18] at $We = 2199$ and $Re_f = 462$–4288.

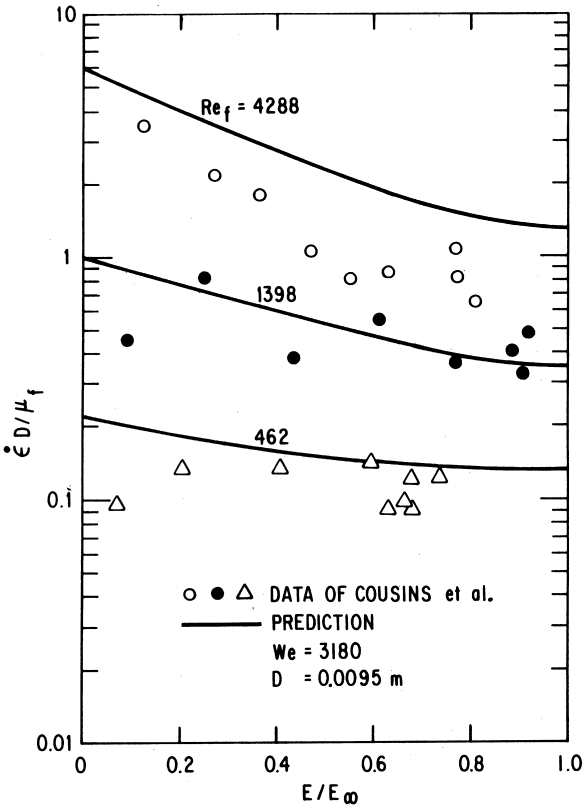

Fig. 5. Entertrainment rate for the data of Cousins et al. [18] at $We = 3180$ and $Re_f = 462$–4288.

The first expression applies to the case when the amount of entrainment is below the equilibrium value, whereas the second expression appliers to the case for $E > E_\infty$. The extra entrainment rate over the equilibrium rate is given by the first term of the right-hand side of Eq. (47). It is proportional to $(Re_{ff} - Re_{ff\infty})^2$ and, therefore, this quantity roughly represents the additional driving force for entrainment through the excess kinetic energy of the film over the equilibrium state. The results seem to be appropriate, since the more the excess kinetic energy is, the more intense the

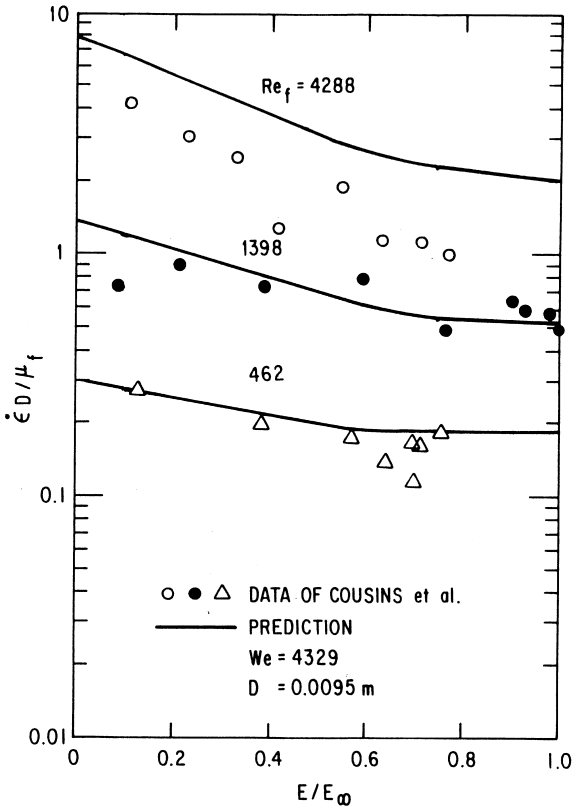

Fig. 6. Entrainment rate for the data of Cousins et al. [18] at $We = 4329$ and $Re_{ff} = 462$–4288.

turbulent level at the interface. This should then lead to an increased entrainment rate when the excess liquid is flowing as a film, i.e., $Re_{ff} \geq Re_{ff\infty}$.

5.2. Entrance effect and experimental data

As indicated by Eq. (18), entrainment rate is obtained by knowing the entrainment amount as a function of the axial distance from the inlet. Cousins et al. [18], Gill and Hewitt [20], and Gill et al. [17] carried out the experiments in which amount of entrainment was measured at various positions from the inlet with relatively smooth injection of liquid as a film [17,18] and with injection of droplets through an axial jet [20]. The amount of entrainment was found to be very sensitive to the inlet conditions. Entrainment rate in the entrance region is considered to be quite different when inlet conditions are different. Because of the differences in the liquid film thickness, the development of the roll wave in the film are supposed to be considerably different, with different inlet conditions.

In collaboration with the data of Cousins et al. [18] and Gill et al. [17], and Eq. (18) the entrainment rate with smooth injection of liquid as a film are obtained. In calculating $\frac{\partial E}{\partial z}$, the gas expansion effect due to axial pressure drop should be carefully distinguished from the entrance effect itself. Therefore, the following procedure of calculation was taken. The amount of entrainment is a function of z and j_g which is a function of z because of gas expansion effects. Then

$$E = E\big(z, j_g(z)\big) \tag{49}$$

Differentiating Eq. (49), one obtains

$$\frac{dE}{dz} = \frac{\partial E}{\partial z} + \frac{\partial E}{\partial j_g}\frac{dj_g}{dz} \tag{50}$$

$$\frac{\partial E}{\partial z} = \frac{dE}{dz} - \frac{\partial E}{\partial j_g}\frac{dj_g}{dz} \tag{51}$$

The right-hand side of Eq. (51) can be calculated by measured entrainment amount and measured pressure drop along the axial position.

Fig. 2 shows $\partial E/\partial z$ calculated by numerically differentiating the data of Cousins et al. [18] and Gill et al.

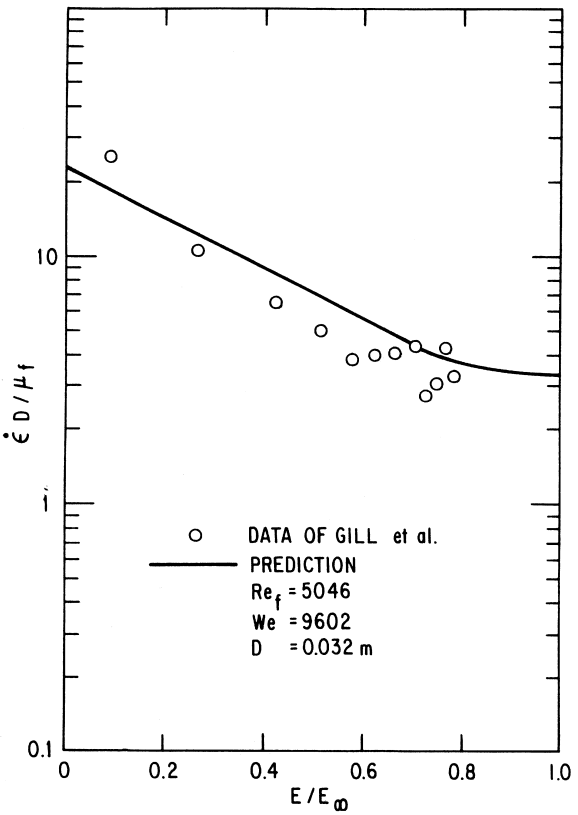

Fig. 7. Entertrainment rate for the data of the Gill et al. [17] at $We = 9602$ and $Re_f = 5046$.

[17]. The solid line in Fig. 2 represents the derivative of Ishii and Mishima's correlation [2] which is given by

$$\frac{\frac{\partial E}{\partial z}DWe^{0.25}}{E_\infty Re_f^{0.5}} = 3.47\times10^{-5}\zeta\exp\left(-1.87\times10^{-5}\zeta^2\right) \quad (52)$$

Although considerably scattered, the data show the general trend predicted by Eq. (52). This scatter comes from the numerical differentiation of the data. As already shown in Ref. [2], the integrated form of Eq. (52), that is Eq. (23), agrees well with the integrated value of the data (entrainment amount).

Figs. 3–7 show some of the entrainment rates obtained from the experimental data of Cousins et al. [18] and Gill et al. [17]. The entrainment rate increases with increasing liquid Reynolds number and with increasing effective Weber number. As for the entrance effects, the entrainment rate increasing with decreasing E/E_∞. This tendency is more eminent for larger Re_f and We. Solid lines in Figs. 3–7 represent Eq. (44) or (47). Although data scatters considerably due to the numerical differentiation, the present correlation well reproduces the experimental trends.

Figs. 8–12 show the comparison of the entrainment rate obtained from the experimental data of

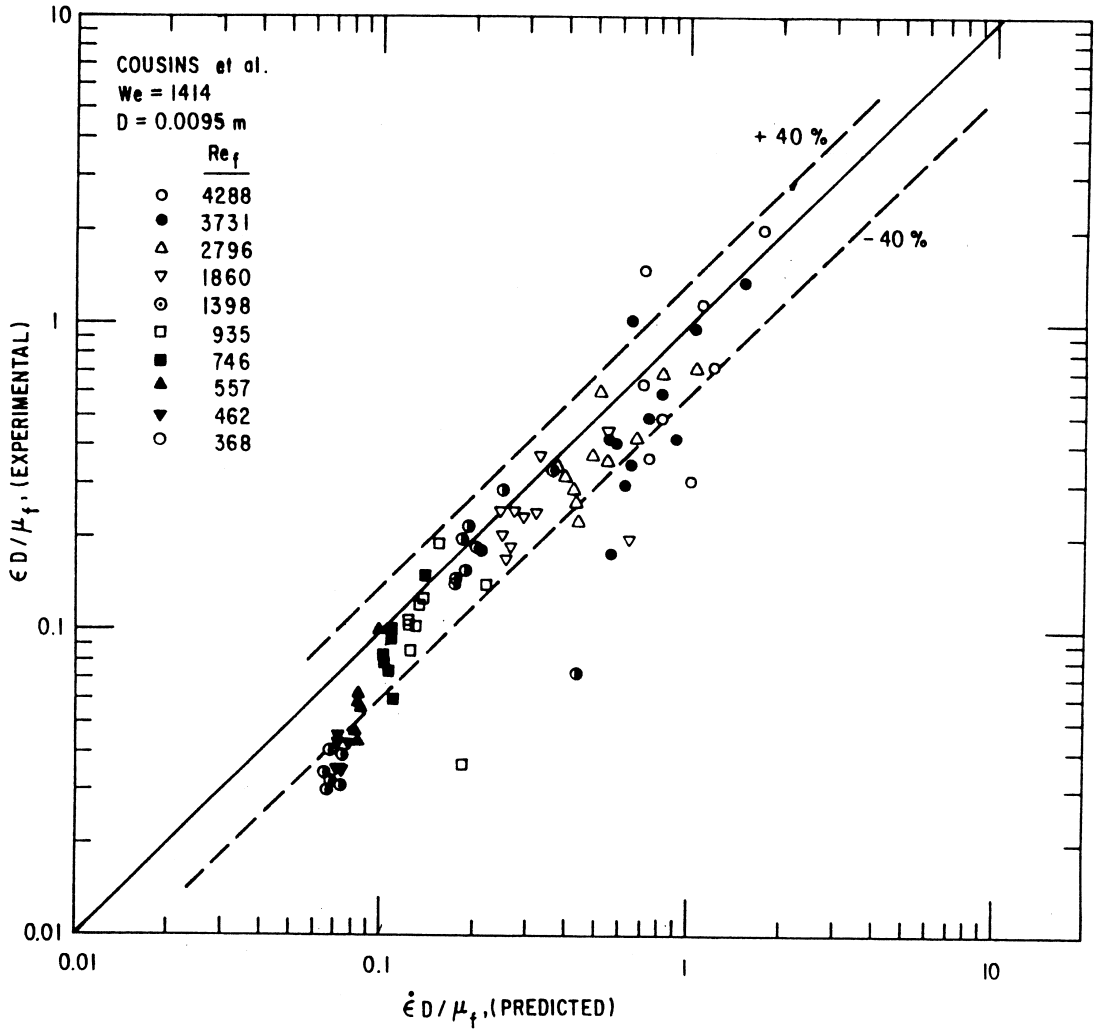

Fig. 8. Comparision of experimental entertrainment rate with Eq. (44) for the data of Cousins et al. [18] at $We = 1414$ and $Re_f = 369$–4288.

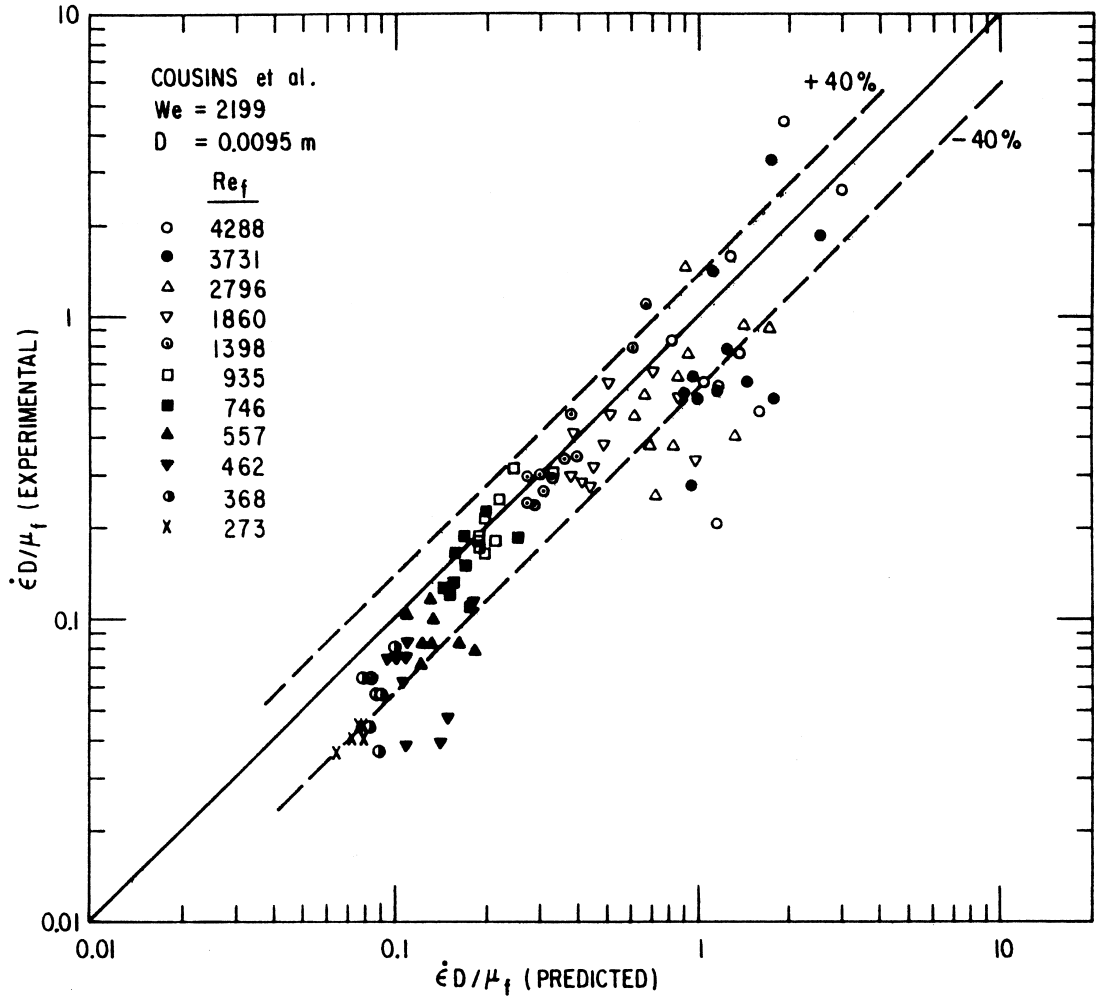

Fig. 9. Comparision of experimental entertainment rate with Eq. (44) for the data of Cousins et al. [18] at $We = 1414$ and $Re_f = 368$–4288.

cousins et al. [18] and Gill et al. [17] with those predicted by Eq. (44). In the ranges of Re_f from 273 to 5041, We from 1414 to 9602, and diameter from 0.0095 to 0.032 m, most of the data fall within ±40% of Eq. (44) or (47).

Now that entrainment rate correlation equation (44) is obtained, one can calculate entrainment amount by integrating the rate equation which is given by

$$\left(\frac{\partial E}{\partial z}\right) = \frac{4}{D\rho_f j_f}(\dot{\varepsilon} - \dot{d}) \tag{53}$$

Substituting Eqs. (17) and (47) into Eq. (53), one obtains for $Re_{ff} \geq Re_{ff\infty}$

$$\begin{aligned}\frac{\partial E}{\partial (z/D)} &= 4.8\times 10^3 Re_f^{-1.5} Re_{ff\infty}^{-0.25} We^{-1.5} \\ &\times (Re_{ff} - Re_{ff\infty})^2 + 2.64\times 10^{-6} Re_f^{-0.26} Re_{ff}^{0.185} We^{0.925} \\ &\times \left(\frac{\mu_g}{\mu_f}\right)^{0.26} - 0.088\, Re_f^{-0.26}\left(\frac{\mu_g}{\mu_f}\right)^{0.26}\left(1 - \frac{Re_{ff}}{Re_f}\right)^{0.74}\end{aligned} \tag{54}$$

And for $Re_{ff} < Re_{ff\infty}$

$$\begin{aligned}\frac{\partial E}{\partial (z/D)} &= 2.64\times 10^{-6} Re_f^{-0.26} Re_{ff}^{0.185} \\ &\times We^{0.925}\left(\frac{\mu_g}{\mu_f}\right)^{0.26} - 0.088 Re_f^{-0.26}\left(\frac{\mu_g}{\mu_f}\right)^{0.26} \\ &\times \left(1 - \frac{Re_{ff}}{Re_f}\right)^{0.74}\end{aligned} \tag{55}$$

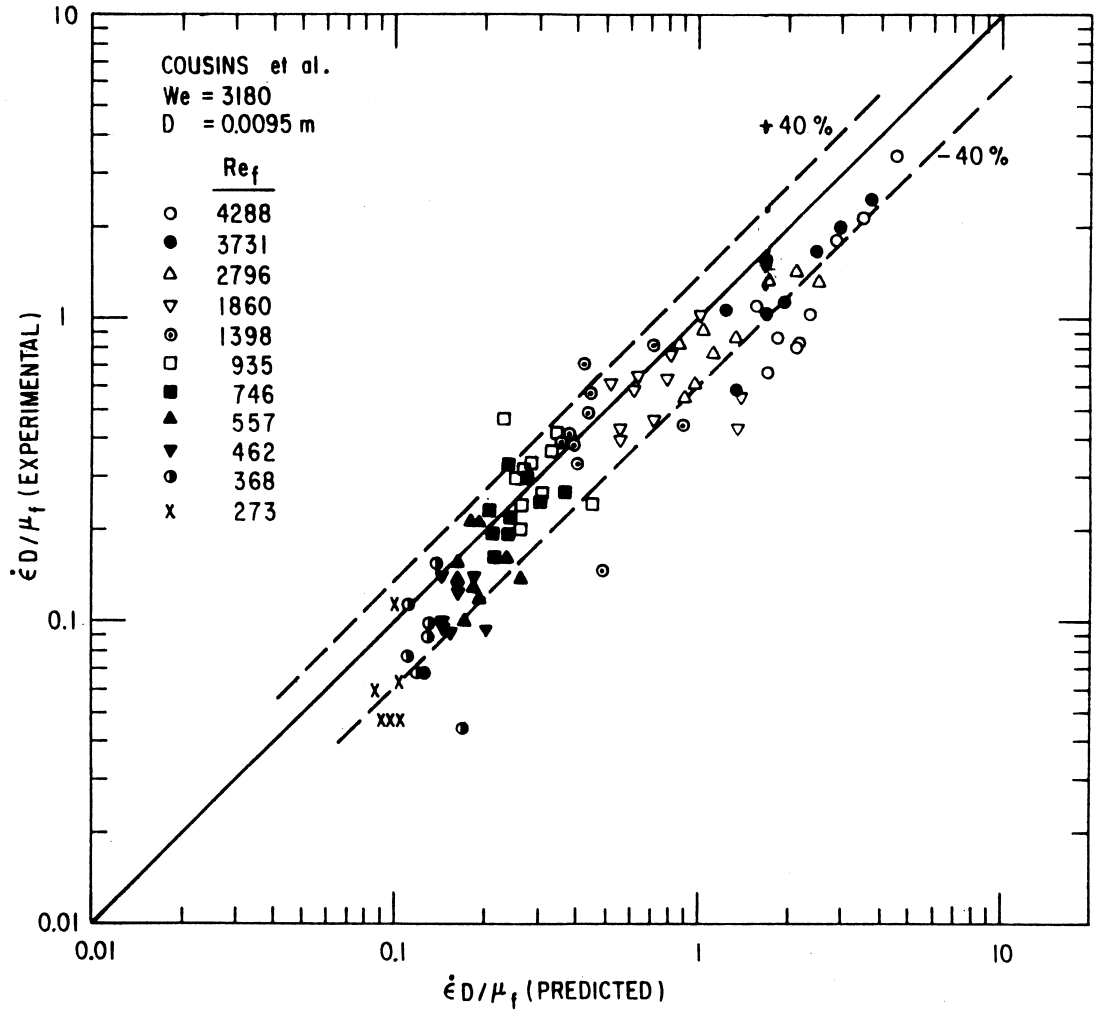

Fig. 10. Comparison of experimental rate with Eq. (44) for the data of Cousins et at. [18] at $We = 3180$ and $Re_f = 273$–4288.

These equations can be rewritten in terms of E as follows. For $E/E_\infty \leq 1$

$$\frac{\partial E}{\partial (z/D)} = 2.87 \times 10^{-9} Re_f^{0.5} Re_{ff\infty}^{0.25} We \left(1 - \frac{E}{E_\infty}\right)^2 + 2.64 \times 10^{-6} Re_f^{-0.075} We^{0.925} \left(\frac{\mu_g}{\mu_f}\right)^{0.26} \times (1-E)^{0.185} - 0.088 Re_f^{-0.26} \left(\frac{\mu_g}{\mu_f}\right)^{0.26} E^{0.74} \quad (56)$$

and $E/E_\infty > 1$

$$\frac{\partial E}{\partial (z/D)} = 2.64 \times 10^{-6} Re_f^{-0.075} We^{0.925} \left(\frac{\mu_g}{\mu_f}\right)^{0.26} \times (1-E)^{0.185} - 0.088 Re_f^{-0.26} \left(\frac{\mu_g}{\mu_f}\right)^{0.26} E^{0.74} \quad (57)$$

Fig. 13 shows the comparison of experimental data of Cousins et al. [18] to the predicted amount of entrainment with the initial condition of $E = 0$ at $z/D = 0$. Except at small Reynolds numbers, the integration of Eq. (54) well reproduces the experimental data. For small Reynolds numbers, however, the experimental data show that it takes a certain distance to inception of entrainment. For the case with the smooth injection of liquid as a film, it should take a certain time for roll waves to grow sufficiently to reach the inception of entrainment. The time required

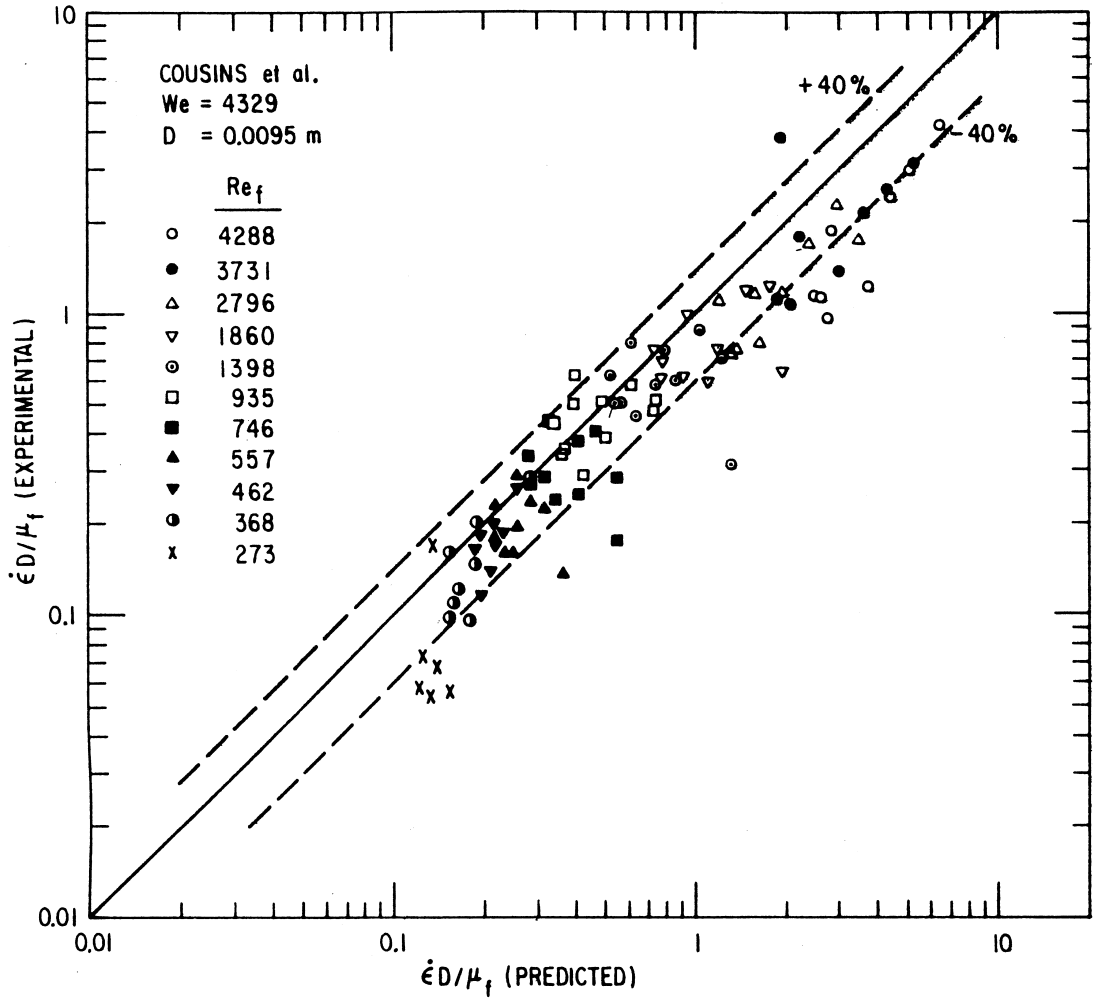

Fig. 11. Comparision of experimental entertainment rate with Eq. (44) for the data Cousins et at. [18] at $We = 4329$ and $Ref = 273$–4288.

should be related to the growth rate of roll wave and the growth rate to some power of $Re_f/\sqrt{We}$ as discussed previously [2]. Therefore, the distance from the inlet without entrainment should be inversely proportional to some power of $Re_f/\sqrt{We}$. The experimental data indicate this trend also at least in the turbulent film flow regime.

Fig. 14 shows the comparison of the experimental data of Gill et al. [17,20] to the predicted amount of entrainment. In their experiment, liquid is introduced by smooth injection as a film ($E = 0$ at $z/D = 0$) or by injection of droplets through an axial jet ($E = 1$ at $z/D = 0$) under the same flow condition. In the case of the smooth injection of liquid, the experimental data agree well with the prediction shown as the solid line. However, in the case of droplet injection, there is a considerable discrepancy between experimental data and the prediction based on the boundary condition of $E = 1$ at $z/D = 0$, shown by the broken line. The experimental data shows there is an abrupt decrease in E between $z/D = 0$ and $z/D = 20$. In this very vicinity of the inlet, the deposition mechanism can be quite different from the diffusion process of droplets which is dominant in the down stream section. The direct droplet impingements and deposition due to the initial droplet momentum at the inlet should play a very important roll in this section [34]. It appears that if the entire liquid is introduced into a system as droplets, this initial deposition rate is very large. Furthermore, it is expected that the rate is strongly dependent on the geometry of the inlet. If this very vicinity of the inlet is excluded, the present model gives reasonable agreement with the data. This can be shown by changing the initial condition from $E = 1.0$ at

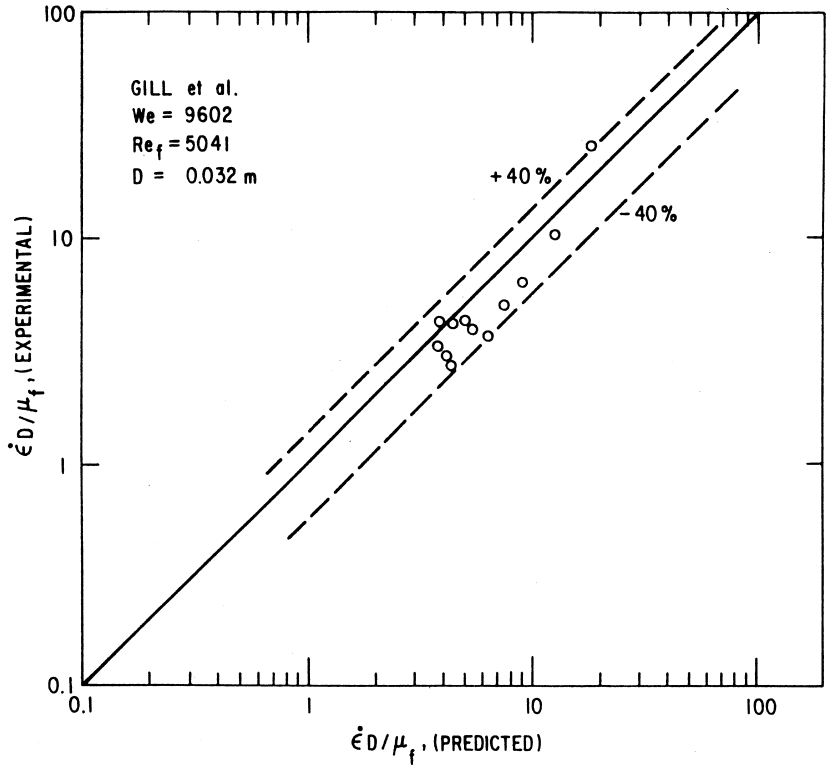

Fig. 12. Comparision of experimental entrainment rate with Eq. (44) for the data for the data of Gill et at. [17] at $We = 9602$ and $Re_f = 5041$.

$z = 0$ to $E = 0.711$ at $z/D = 20$. The result shown in Fig. 14 as a dotted line seems to be quite satisfactory.

The rough estimate of this geometry dependent inlet section can be obtained from the previously developed correlation for the amount of entrainment. It is thought that the full entrainment process is reached when the above mentioned entrainment rate function $f(E/E_\infty)$ reaches to its maximum value (see Eq. (41)). From this, the geometry dependent inlet region is given by

$$0 \le z \le 160 D We^{0.25} Re_f^{-0.5} \tag{58}$$

The comparison of the data to the above inequality indicates that it gives a reasonable criterion. However, at very small Reynolds numbers, the phenomena seems to be more complicated than that predicted by Eq. (58).

6. Summary and conclusions

A correlation for the rate of entrainment in annular flow has been developed from a simple model and experimental data. The previously developed correlation for the amount of entrainment has been used as a basis of the present study. The amount of entrainment represents the integrated effect of the local rate processes of entrainment and deposition. The entrainment rate and deposition rate are more mechanistic parameters representing the true transfer of liquid mass at the wavy interfaces than is the entrainment amount. However, because of that these rates are much more difficult parameters to measure and correlate.

The present correlation indicates that the entrainment rate depends on the total liquid Reynolds number, Weber number, equilibrium entrainment fraction E and entrainment fraction E or the local film Reynolds number. These correlations are compared to a number of experimental data both in terms of the entrainment rate and entrainment fraction. The results are shown to be satisfactory both in the developing region and fully developed entrainment region.

The present model is based on the previously developed criteria for the onset of entrainment and the correlation for the entrainment fraction. Since these are developed from a simple model based on the

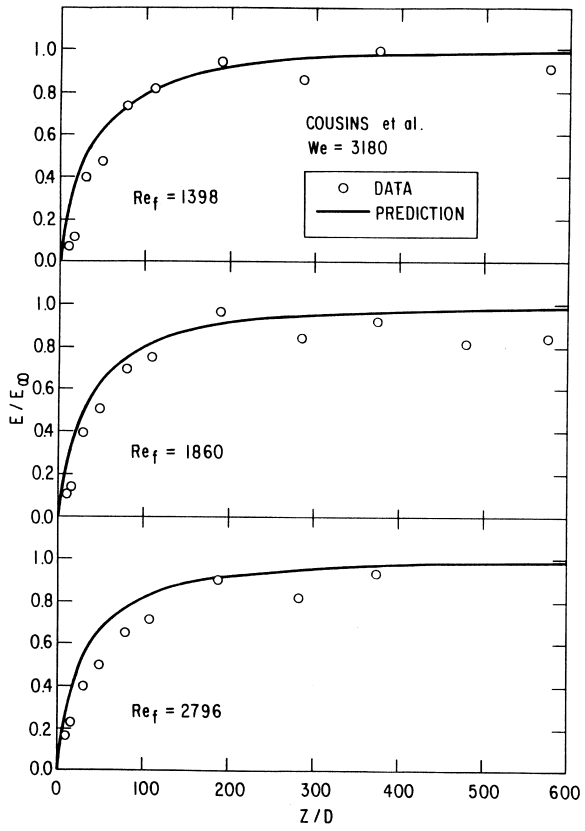

Fig. 13. Comparision of experimental data of Cousins et al. [18] with predicated amount of entrainment at $We = 3180$ and $Re_f = 1398$–2796.

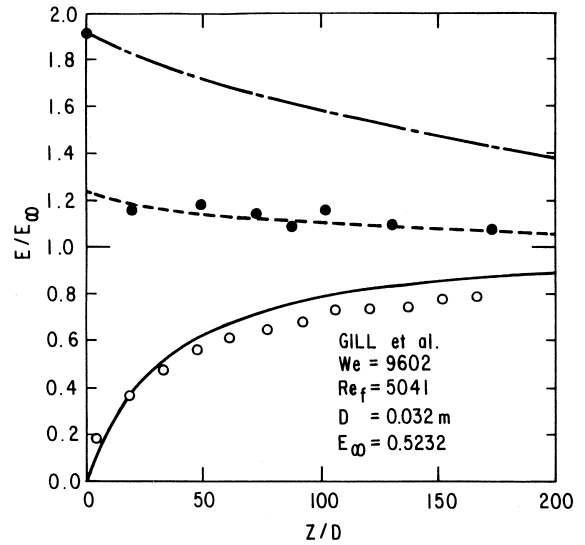

Fig. 14. Comparison of experimental data of Gill et al. [17] with predicted amount of entertrainment at $We = 9602$ and $Re_f = 5041$.

force balance at the wavy interface, the present correlation for entrainment rate indicates basic mechanisms of entrainment processes and parametric dependencies in addition to being accurate. The entrainment rate correlation in the developing region is completely new. Therefore, the present results supply very valuable information which has not been available previously.

Acknowledgements

The authors would like to express their appreciation to Drs. N. Zuber and Y.Y. Hsu of NRC for valuable discussions on the subject. This work was performed under the auspices of the U.S. Nuclear Regulatory Commission.

References

[1] G.F. Hewitt, N.S. Hall-Taylor, Annular Two-phase Flow, Pergamon Press, Oxford, 1970.
[2] M. Ishii, K. Mishima, Correlation for liquid entrainment in annular two-phase flow of low viscous fluid, Argonne National Laboratory Report, ANL/RAS/LWR 81-2, 1981.
[3] J.G. Collier, Burnout in liquid cooled reactors, Nuclear Power 5 (1961) 61.
[4] V.I. Petrovichev, L.S. Kokorev, A.Ya. Didenko, G.P. Dubvrovskiy, Droplet entrainment in boiling of thin liquid film, Heat Transfer—Soviet Res. 3 (1971) 19.
[5] L.B. Cousins, W.H. Denton, G.E. Hewitt, Liquid mass transfer in annular two-phase flow, in: Sym. on Two-phase Flow, vol. 1, paper C4, Exeter, England, 1965.
[6] L.S. Tong, Boiling Heat Transfer and Two-phase Flow, Krieger, New York, 1975.
[7] Y.Y. Hsu, R.W. Graham, R.W. Graham, Transport Process in Boiling and Two-phase Systems, Hemisphere, Washington, DC, 1976.
[8] G.F. Hewitt, Mechanism and prediction of burnout, NATO Advanced Study Institute on Two Phase Flows, 1976.
[9] A. Yamanouchi, Effects of core spray cooling at stationary state after loss of coolant accident, J. Nuc. Sci. and Tech. 5 (9) (1968) 498.
[10] R. Semeria, Martinet, calefaction spots on a heating wall; temperature distribution and resorption. Sym. on boiling heat transfer in steam generating unit and heat exchangers, Proc. Inst. Mech. Engs 180 (1965) 192–205.
[11] R. Duffey, The physics of rewetting in water reactor emergency core cooling, Nucl. Eng. Design 25 (1973) 379.
[12] A. Bennett, The wetting of hot surfaces by water in a steam environment at high pressure, Atomic Energy Research Establishment, Harwell, AERE-R5146, 1966.
[13] M. Ishii, M.A. Grolmes, Inception criteria for droplet

entrainment in two-phase concurrent film flow, AIChE J 21 (1975) 21.

[14] I. Kataoka, M. Ishii, K. Mishima, Generation and size distribution of droplet in gas–liquid annular two-phase flow, Argonne National Laboratory Report, ANL/RAS/LWR 81-3, 1981.

[15] L.G. Alexander, C.L. Coldren, Droplet transfer from suspending air to duct walls, Ind. Eng. Chem 43 (1951) 1325.

[16] K. Goldman, H. Firstenberg, C. Lombardi, Burnout in turbulent flow: a droplet diffusion model, Trans. ASME J. Heat Trans 83 (1961) 158.

[17] L.E. Gill, G.F. Hewitt, J.W. Hitchon, Sampling probe studies of the gas core in annular two-phase flow. Part I: the effect of length on phase and velocity distribution, AERE-R 3954, 1962.

[18] L.B. Cousins, W.H. Denton, G.F. Hewitt, Liquid mass transfer in annular two-phase flow, in: Sym. on Two-phase Flow, vol. 1, paper C4, Exeter, England, 1965.

[19] I.I. Paleev, B.S. Filippovich, Phenomena of liquid transfer in two-phase dispersed annular flow, Int. J. Heat Mass Trans 9 (1966) 1089.

[20] L.E. Gill, G.F. Hewitt, Sampling probe studies of the gas core in annular two-phase flow. Part III: distribution of velocity and droplet flow-rate after injection through an axial jet, AERE-M1202, 1967.

[21] L.E. Gil, G.F. Hewitt, Sampling probe studies of the gas core in annular two-phase flow—III: distribution of velocity and droplet flowrate after injection through an axial jet, Chem. Eng. Sci. 23 (1968) 677.

[22] L.B. Cousins, G.F. Hewitt, Liquid phase mass transfer in annular two-phase flow: radial liquid mixing, AERE-R5693, 1968.

[23] L.B. Cousins, G.F. Hewitt, Liquid phase mass transfer in annular two-phase flow: droplet deposition and liquid entrainment, AERE-R5657, 1968.

[24] P. Hutchinson, G.F. Hewitt, A.E. Dukler, Deposition of liquid on solid dispersion from turbulent gas streams: a stochastic model, Chem. Eng. Sci. 26 (1971) 419.